

# Selective NO<sub>x</sub> reduction during the H<sub>2</sub> + NO + O<sub>2</sub> reaction under oxygen-rich conditions over Pd/V<sub>2</sub>O<sub>5</sub>/Al<sub>2</sub>O<sub>3</sub>: evidence for *in situ* ammonia generation

Norman Macleod and Richard M. Lambert\*

Department of Chemistry, University of Cambridge, Lensfield Rd, Cambridge CB2 1EW, UK

Received 20 May 2003; accepted 5 August 2003

Under oxygen-rich conditions in H<sub>2</sub> + NO + O<sub>2</sub> mixtures, Pd/V<sub>2</sub>O<sub>5</sub>/Al<sub>2</sub>O<sub>3</sub> catalysts are active and highly selective (~80%) for NO<sub>x</sub> reduction to N<sub>2</sub>. *In situ* DRIFT spectroscopy and reactor data show that the system operates via formation of NH<sub>x</sub> species on the highly dispersed V<sub>2</sub>O<sub>5</sub> component. Both NH<sub>3</sub> and NH<sub>4</sub><sup>+</sup> are formed, with the latter dominant. The role of the palladium component is also discussed.

**KEY WORDS:** NO; palladium; H<sub>2</sub>; N<sub>2</sub>O; lean burn; Al<sub>2</sub>O<sub>3</sub>; V<sub>2</sub>O<sub>5</sub>; FTIR; DRIFTS.

## 1. Introduction

Catalytic reduction of the nitrogen oxides (NO, NO<sub>2</sub>) produced by lean burn gasoline and diesel engines is problematic due to the very high oxygen concentrations present in the exhaust streams. This makes effective utilization of any available reductants (HC, CO, H<sub>2</sub>) for NO<sub>x</sub> removal extremely difficult, as these species are consumed preferentially by reaction with O<sub>2</sub> [1,2]. The control of NO<sub>x</sub> emissions from stationary power sources and various chemical plants is also environmentally important. For these applications, the NH<sub>3</sub> SCR process [3,4], employing V<sub>2</sub>O<sub>5</sub>/TiO<sub>2</sub>-based catalysts, is currently the most widely used option for NO<sub>x</sub> abatement. Ammonia is employed as it displays very high selectivity toward NO<sub>x</sub> even under these highly oxygen-rich conditions. Although very effective, the requirement for a separate NH<sub>3</sub> reservoir and injection system disfavors the use of this technology for transport applications. Safer alternatives such as urea, the decomposition of which can be used to make ammonia, have therefore been extensively studied [5–7]. Strategies for onboard NH<sub>3</sub> formation have also been discussed [8].

Recently, we showed that Pd/TiO<sub>2</sub> catalysts can generate NH<sub>3</sub> *in situ* when fed with H<sub>2</sub> + NO + O<sub>2</sub> under oxygen-rich conditions, resulting in very high NO<sub>x</sub> conversions (70–80%) being attained [9]. The high activity of Pd/TiO<sub>2</sub> under these conditions was first reported by Ueda *et al.* [10,11]. Two separate pathways for NO<sub>x</sub> reduction were observed, operating at different temperatures. Employing *in situ* diffuse reflectance infrared Fourier transform spectroscopy (DRIFTS) [9],

we were able to assign the low-temperature process at ~120 °C (the temperature region where H<sub>2</sub> conversion approaches 100%) to dissociation and reaction of NO on reduced (Pd<sup>0</sup>) metal sites. In contrast, the high-temperature mechanism at ~240 °C was shown to operate via the formation and subsequent reaction of NH<sub>3</sub>. A similar mechanism was recently proposed by Burch and Coleman to account for the promoting influence of MoO<sub>3</sub> in Pt/MoO<sub>3</sub>/Al<sub>2</sub>O<sub>3</sub> catalysts during the H<sub>2</sub>/NO/O<sub>2</sub> reaction under oxygen-rich conditions [12].

In this paper, we report on the H<sub>2</sub> + NO + O<sub>2</sub> reaction over a Pd/V<sub>2</sub>O<sub>5</sub>/Al<sub>2</sub>O<sub>3</sub> catalyst. This system has been studied by a combination of reactor measurements and DRIFT spectroscopy. It is shown that at temperatures above 200 °C, the Pd/V<sub>2</sub>O<sub>5</sub>-based system performs in a similar manner to that reported previously for Pd/TiO<sub>2</sub>-generating NH<sub>x</sub> species *in situ*, which subsequently result in very high NO<sub>x</sub> conversions being attained. Indeed, the V<sub>2</sub>O<sub>5</sub>-based catalyst was found to deliver significantly improved NO<sub>x</sub> conversion (~90%) compared to that observed previously with Pd/TiO<sub>2</sub> (~70%) in this temperature range. The separate roles of the palladium and V<sub>2</sub>O<sub>5</sub> components of the Pd/V<sub>2</sub>O<sub>5</sub>/Al<sub>2</sub>O<sub>3</sub> catalyst in the reaction mechanism are also discussed.

## 2. Experimental

The 10 wt% V<sub>2</sub>O<sub>5</sub>/Al<sub>2</sub>O<sub>3</sub> support was prepared by hydrolysis of vanadium (V) oxytriisopropoxide in the presence of the alumina support, in a manner similar to that used previously to prepare mixed TiO<sub>2</sub>/Al<sub>2</sub>O<sub>3</sub> catalysts [13,14]. The resulting solid material was then

\* To whom correspondence should be addressed.  
E-mail: rml1@cam.ac.uk

calcined in air at  $500^\circ\text{C}$  for 10 h. An XRD pattern obtained from the  $\text{V}_2\text{O}_5/\text{Al}_2\text{O}_3$  sample at this stage displayed a profile identical to that of  $\gamma\text{-Al}_2\text{O}_3$ , indicating that the vanadium component was very highly dispersed. Palladium was subsequently added by impregnation with an aqueous solution of palladium (II) nitrate sufficient to yield 0.5 wt% metal loading. Following impregnation, the catalyst was dried in air overnight at  $110^\circ\text{C}$ , calcined once again in air at  $500^\circ\text{C}$  for 6 h and subsequently crushed/sieved to yield grain sizes in the range  $255\text{--}350\ \mu\text{m}$ . A 0.5 wt%  $\text{Pd}/\text{Al}_2\text{O}_3$  catalyst was prepared in a similar manner. Metal dispersion was determined using the CO methanation technique [15], assuming a 1:1 CO to surface metal atom ratio. The dispersions measured were 47 and 30% for  $\text{Pd}/\gamma\text{-Al}_2\text{O}_3$  and  $\text{Pd}/\text{V}_2\text{O}_5/\text{Al}_2\text{O}_3$ , respectively.

Catalyst testing was performed in a quartz micro-reactor system described previously [15]. The gas feed composition consisted of 4000 ppm  $\text{H}_2$ , 500 ppm NO and 5%  $\text{O}_2$ , delivered to the reactor with a total flow of  $200\ \text{mL min}^{-1}$ . A sample weight of 100 mg was employed, corresponding to a reciprocal weight time velocity of  $w/f = 0.03\ \text{g s mL}^{-1}$ . Prior to testing, the samples were calcined in air ( $60\ \text{mL min}^{-1}$ ) for 6 h at  $500^\circ\text{C}$ . The reactor outflow was analyzed using a chemiluminescence  $\text{NO}_x$  ( $\text{NO} + \text{NO}_2$ ) analyzer (Signal 4000 series) and a dual channel NDIR detector (Siemens Ultramat 6) calibrated for  $\text{NO}/\text{N}_2\text{O}$ . Hydrogen consumption was monitored via a quadrupole mass spectrometer (Hiden RGA 301). Nitrogen production was calculated by subtracting the  $\text{N}_2\text{O}$  contribution from the total  $\text{NO}_x$  conversion. (Gas Chromatography (GC) analysis produced no evidence for  $\text{NH}_3$  in the reactor outlet during these experiments). The catalyst temperature and all analyzer outputs were continuously monitored and recorded by a PC. Light-off profiles, typically containing 1000 data points per channel, were obtained as the catalyst temperature was raised from  $50\text{--}450^\circ\text{C}$  with a linear ramp of  $2\ \text{K min}^{-1}$ .

DRIFTS experiments were performed with a Perkin–Elmer GX2000 spectrometer equipped with an MCT detector and a high-temperature, high-pressure DRIFTS cell (Thermo Spectra-Tech) fitted with ZnSe windows. Spectra were acquired at a resolution of  $4\ \text{cm}^{-1}$  typically averaging 32 scans. Background spectra were obtained from samples at the relevant temperature in a flow of 5% oxygen.

### 3. Results and discussion

#### 3.1. Catalyst activity

Conversion versus temperature profiles for the reduction of NO by hydrogen (4000 ppm  $\text{H}_2$  + 500 ppm NO + 5%  $\text{O}_2$ ) over the 0.5 wt%  $\text{Pd}/10\ \text{wt}\% \text{V}_2\text{O}_5/\text{Al}_2\text{O}_3$  catalyst are displayed in figure 1. A maximum  $\text{NO}_x$  conversion of 95% was achieved at

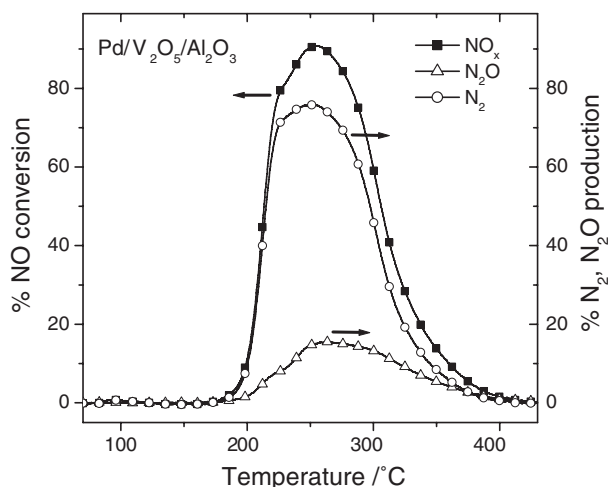


Figure 1. Total NO conversion and  $\text{N}_2/\text{N}_2\text{O}$  yields as a function of temperature during NO reduction by  $\text{H}_2$  over  $\text{Pd}/\text{V}_2\text{O}_5/\text{Al}_2\text{O}_3$  (4000 ppm  $\text{H}_2$  + 500 ppm NO + 5%  $\text{O}_2$ ).

$250^\circ\text{C}$  with this sample. Under identical conditions, with the corresponding  $\text{Pd}/\text{Al}_2\text{O}_3$  catalyst, the  $\text{NO}_x$  conversion did not exceed 10% [9]. It is therefore clear, that addition of  $\text{V}_2\text{O}_5$  to this system strongly influences its performance. Very high  $\text{NO}_x$  conversions were maintained over a relatively wide temperature range, with  $>80\%$  conversion observed between  $225$  and  $280^\circ\text{C}$ . The nitrogen selectivity (defined as  $\%S_{\text{N}_2} = [\text{N}_2]/([\text{N}_2] + [\text{N}_2\text{O}]) \times 100$ ) obtained over this catalyst was also high, with  $\%S_{\text{N}_2} = 81\%$  at the temperature of the conversion maximum. Although the  $\text{NO}_x$  conversion observed over  $\text{Pd}/\text{V}_2\text{O}_5/\text{Al}_2\text{O}_3$  was significantly higher than that reported previously over  $\text{Pd}/\text{TiO}_2$  ( $\sim 70\%$ ) under these conditions [9], the hydrogen light-off occurred at a somewhat higher temperature on the  $\text{V}_2\text{O}_5$  containing sample, with 100%  $\text{H}_2$  conversion not attained until  $180^\circ\text{C}$  as compared to  $110^\circ\text{C}$  over  $\text{Pd}/\text{TiO}_2$ . Therefore, the low-temperature  $\text{NO}_x$  reduction pathway observed on  $\text{Pd}/\text{TiO}_2$  was not seen with  $\text{Pd}/\text{V}_2\text{O}_5/\text{Al}_2\text{O}_3$ . It is important to note that when the  $\text{H}_2 + \text{NO} + \text{O}_2$  reaction was carried out over a  $\text{V}_2\text{O}_5/\text{Al}_2\text{O}_3$  sample in the absence of Pd, very low  $\text{NO}_x$  conversions were observed, indicating the key role of palladium in the reaction mechanism.

#### 3.2. Characterization of adsorbed $\text{NO}_x$ species by DRIFTS

DRIFT spectra obtained in a flow containing NO +  $\text{O}_2$  (500 ppm NO + 5%  $\text{O}_2$ ) over  $\text{Pd}/\text{Al}_2\text{O}_3$ ,  $\text{Pd}/10\ \text{wt}\% \text{V}_2\text{O}_5/\text{Al}_2\text{O}_3$ , and  $\text{V}_2\text{O}_5/\text{Al}_2\text{O}_3$  samples at various temperatures are shown in figure 2(a), (b), and (c), respectively. The various bands at  $1615\text{--}1550\ \text{cm}^{-1}$  and  $1305\text{--}1225\ \text{cm}^{-1}$  observed over  $\text{Pd}/\text{Al}_2\text{O}_3$  may be assigned with confidence to the asymmetric and symmetric stretching modes respectively of variously co-ordinated alumina-bound nitrates [16–18]. In contrast, only very weak nitrate bands at  $1595$  and  $1294\ \text{cm}^{-1}$  (not

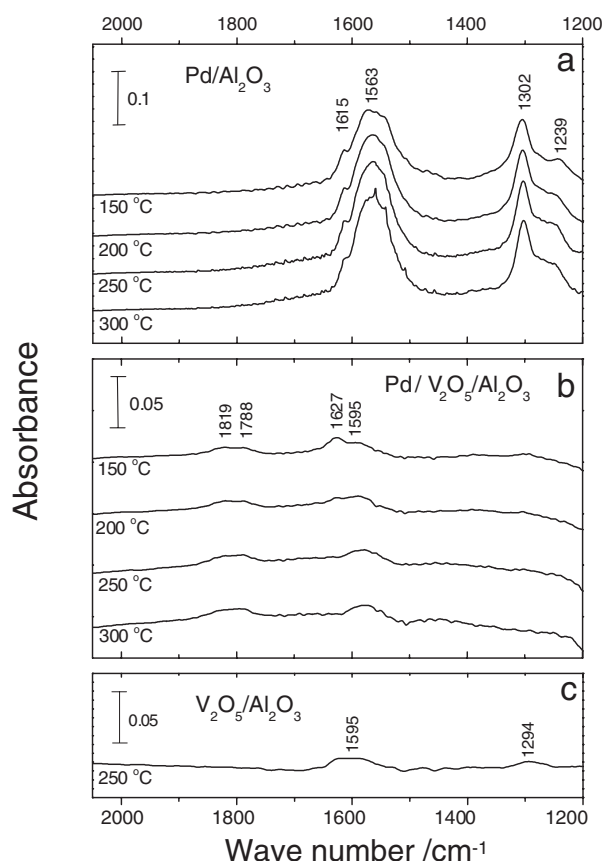


Figure 2. DRIFT spectra obtained at various temperatures in a flow containing  $\text{NO} + \text{O}_2$  over (a)  $\text{Pd}/\text{Al}_2\text{O}_3$ , (b)  $\text{Pd}/\text{V}_2\text{O}_5/\text{Al}_2\text{O}_3$  and (c)  $\text{V}_2\text{O}_5/\text{Al}_2\text{O}_3$ . Each temperature maintained for 1 h prior to recording spectra (500 ppm  $\text{NO} + 5\%$ ).

resolved in all the spectra) were observed with the 10 wt%  $\text{V}_2\text{O}_5/\text{Al}_2\text{O}_3$  containing samples (note different scales). This indicates almost complete coverage of the alumina surface by  $\text{V}_2\text{O}_5$  at this loading. A new band observed at  $1627\text{ cm}^{-1}$  on the  $\text{V}_2\text{O}_5$ -containing sample is assigned to a  $\text{NO}_2$  species adsorbed on  $\text{V}_2\text{O}_5$  sites [19–22]. The intensity of this feature decreased as the temperature increased and it was not observed above  $250\text{ }^\circ\text{C}$ . On  $\text{Pd}/\text{V}_2\text{O}_5/\text{Al}_2\text{O}_3$ , further relatively weak bands were observed at 1819 and  $1788\text{ cm}^{-1}$ . These bands are in the region expected for nitrosyl species. The fact that these features were not observed on the  $\text{V}_2\text{O}_5/\text{Al}_2\text{O}_3$  sample, figure 2(c) suggests that they are related to  $\text{NO}$  adsorbed on the palladium component, with the stretching frequencies being closest to those expected for  $\text{NO}$  adsorbed on  $\text{Pd}^+$  sites [9,19,23,24]. Note that in regard to this assignment, vanadium mono- and dinitrosyl species, which also adsorb in this frequency range, are only observed on  $\text{V}_2\text{O}_5$ -containing catalysts following reductive treatments that result in production of  $\text{V}^{4+}$  and  $\text{V}^{3+}$  sites [25–28] ( $\text{V}^{5+}$  ( $d^0$ ) does not adsorb  $\text{NO}$  [19,29]). As our  $\text{Pd}/\text{V}_2\text{O}_5/\text{Al}_2\text{O}_3$  catalyst was calcined in air at  $500\text{ }^\circ\text{C}$  prior to its contact with  $\text{NO} + \text{O}_2$ , the presence of reduced vanadium centers is extremely unlikely.

### 3.3. DRIFTS of $\text{Pd}/\text{V}_2\text{O}_5/\text{Al}_2\text{O}_3$ under reaction conditions

The corresponding DRIFT spectra obtained in the presence of hydrogen ( $4000\text{ ppm H}_2 + 500\text{ ppm NO} + 5\%\text{ O}_2$ ) over  $\text{Pd}/\text{V}_2\text{O}_5/\text{Al}_2\text{O}_3$  are shown in figure 3. At  $150\text{--}200\text{ }^\circ\text{C}$  in flowing  $\text{H}_2 + \text{NO} + \text{O}_2$  bands due to  $\text{Pd}^+ - \text{NO}$  species ( $1819/1788\text{ cm}^{-1}$ ), adsorbed  $\text{NO}_2$  ( $1623\text{ cm}^{-1}$ ) and nitrate ( $1587\text{ cm}^{-1}$ ) were again observed. However, at  $250\text{ }^\circ\text{C}$ , the temperature of the conversion maximum in figure 1, these bands disappeared and were replaced by bands at 1660, 1625, 1420, and  $1282\text{ cm}^{-1}$ . The bands at 1660 and  $1420\text{ cm}^{-1}$  are assigned to the symmetric and asymmetric bending modes of  $\text{NH}_4^+$ , whilst the bands at 1625 and  $1282\text{ cm}^{-1}$  are assigned to the corresponding deformation modes of adsorbed  $\text{NH}_3$  [19–29, 30–32]. These assignments are confirmed by the appearance of the corresponding N-H stretching modes at  $3400\text{--}3170\text{ cm}^{-1}$  for  $\text{NH}_3$  and broadbands at 3020 and  $2810\text{ cm}^{-1}$  for  $\text{NH}_4^+$  (not shown). By comparing the intensities of the bands at 1420 and  $1282\text{ cm}^{-1}$ , it is clear that the  $\text{Pd}/\text{V}_2\text{O}_5/\text{Al}_2\text{O}_3$  catalyst contained a much greater concentration of Brønsted than Lewis acid sites.

A negative band also developed at  $2045\text{ cm}^{-1}$  at  $250\text{ }^\circ\text{C}$ . This feature is assigned to the first overtone vibration of  $\text{V}^{5+} = \text{O}$  groups [21,22,27,29,32,33] and is characteristic of the presence of  $\text{V}_2\text{O}_5$ . This loss of  $\text{V} = \text{O}$  species under these conditions is due to their reduction by ammonia [27] (note that these spectra were obtained by ratioing with reference spectra taken in a flow of oxygen). As the temperature was raised further, the intensity of the  $\text{NH}_4^+$  and  $\text{NH}_3$  bands decreased, mirroring the decline in activity that occurred above  $250\text{ }^\circ\text{C}$ , and the  $\text{Pd}^+ - \text{NO}$  bands at 1820 and  $1788\text{ cm}^{-1}$  reappeared. At these higher temperatures, the negative

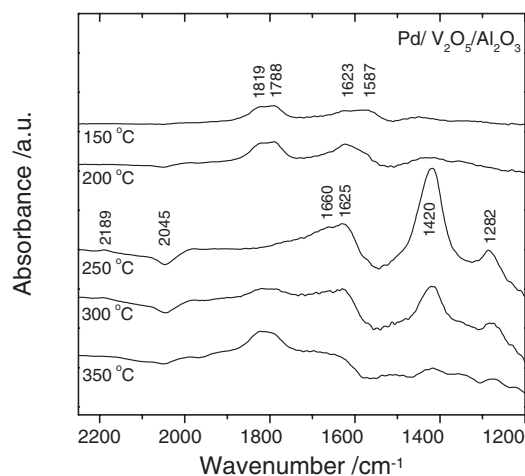


Figure 3. DRIFT spectra obtained at various temperatures in a flow containing  $\text{H}_2 + \text{NO} + \text{O}_2$  over  $\text{Pd}/\text{V}_2\text{O}_5/\text{Al}_2\text{O}_3$ . Each temperature maintained for 1 h prior to recording spectra ( $4000\text{ ppm H}_2 + 500\text{ ppm NO} + 5\%\text{ O}_2$ ).



peak at  $2045\text{ cm}^{-1}$  was also removed because of reoxidation of vanadium.

To investigate the uptake and reactivity of the  $\text{NH}_x$  species, time-resolved DRIFTS studies were performed. The time-resolved spectra obtained over the  $\text{Pd}/\text{V}_2\text{O}_5/\text{Al}_2\text{O}_3$  catalyst at  $250^\circ\text{C}$  following the switch from a flow containing 500 ppm  $\text{NO} + 5\%\text{O}_2$  to a flow containing 4000 ppm  $\text{H}_2 + 500\text{ ppm NO} + 5\%\text{O}_2$  are shown in figure 4. The surface concentration of  $\text{NH}_4^+$  ( $1660/1420\text{ cm}^{-1}$ ) and  $\text{NH}_3$  ( $1625/1288\text{ cm}^{-1}$ ) species increased rapidly and reached steady state after  $\sim 20$  min. Loss of the  $\text{Pd}^+ - \text{NO}$  peaks at  $\sim 1819\text{ cm}^{-1}$  was observed during this time along with the appearance of the negative band at  $2045\text{ cm}^{-1}$  associated with the removal of  $\text{V}^{5+} = \text{O}$  groups. An additional weak band also developed at  $2189\text{ cm}^{-1}$ . A similar band was observed at  $2180\text{ cm}^{-1}$  by Ramis *et al.* [31] following adsorption of  $\text{NH}_3$  on a  $\text{CuO}/\text{TiO}_2$  catalyst at room temperature and outgassing at  $250^\circ\text{C}$ . This was assigned to a dinitrogen anion species,  $\text{N}_2^-$ . Adsorption of  $\text{NH}_3$  on  $\text{TiO}_2$  followed by outgassing to various temperatures also produced a band in this range ( $2197\text{ cm}^{-1}$ ), which was again assigned to a  $\text{N}_2^-$  species [34]. However, an alternative assignment of this band to a  $\text{NO}^+$  species is also possible [19].

Following the accumulation of the  $\text{NH}_x$  species as shown in figure 4, their reactivity toward  $\text{NO} + \text{O}_2$  was subsequently studied by removing the  $\text{H}_2$  component from the gas mix. The resultant time-resolved data obtained following the switch in gas feed from 4000 ppm  $\text{H}_2 + 500\text{ ppm NO} + 5\%\text{O}_2$  to 500 ppm  $\text{NO} + 5\%\text{O}_2$  are shown in figure 5. The intensity of the bands associated with both  $\text{NH}_3$  and  $\text{NH}_4^+$  declined very rapidly during the first 5 min following removal of hydrogen and more gradually thereafter. This indicates that both  $\text{NH}_3$  and  $\text{NH}_4^+$  are readily consumed in the presence of  $\text{NO} + \text{O}_2$ . It should be noted that on a corresponding  $\text{Pd}/\text{TiO}_2$  catalyst, the major  $\text{NH}_x$  species observed under

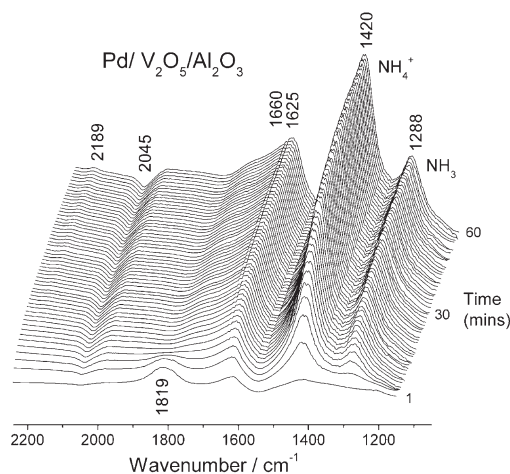


Figure 4. Time-resolved DRIFT spectra showing accumulation of  $\text{NH}_3$  and  $\text{NH}_4^+$  species in a flow containing  $\text{H}_2 + \text{NO} + \text{O}_2$  flow over  $\text{Pd}/\text{V}_2\text{O}_5/\text{Al}_2\text{O}_3$  at  $250^\circ\text{C}$  (4000 ppm  $\text{H}_2 + 500\text{ ppm NO} + 5\%\text{O}_2$ ).

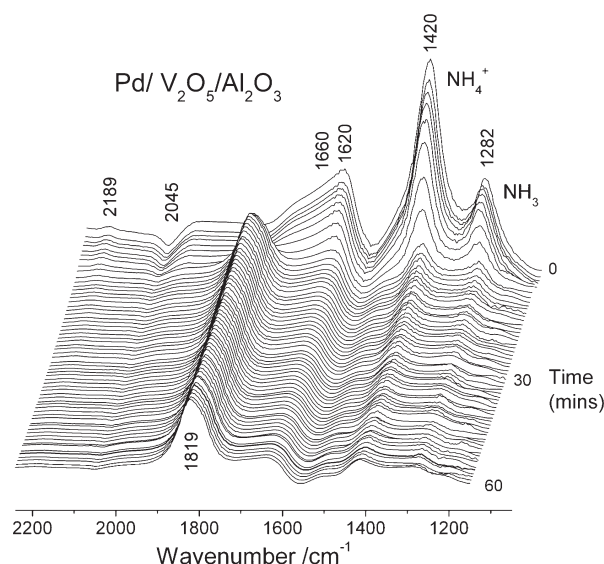


Figure 5. Time-resolved DRIFT spectra showing reactivity of  $\text{NH}_3$  and  $\text{NH}_4^+$  species in flowing  $\text{NO} + \text{O}_2$  over  $\text{Pd}/\text{V}_2\text{O}_5/\text{Al}_2\text{O}_3$  at  $250^\circ\text{C}$  (500 ppm  $\text{NO} + 5\%\text{O}_2$ ).

reaction conditions was  $\text{NH}_3$  coordinated on Lewis acid sites, with only a very minor concentration of  $\text{NH}_4^+$  being observed [9]. Following the switch to  $\text{NO} + \text{O}_2$ , the intensity of the negative band at  $2045\text{ cm}^{-1}$  assigned to loss of  $\text{V}^{5+} = \text{O}$  groups decreased significantly, indicating reoxidation of vanadium. The weak band at  $2185\text{ cm}^{-1}$  ( $\text{N}_2^-$  or  $\text{NO}^+$ ) was also rapidly extinguished. The bands at  $\sim 1819\text{ cm}^{-1}$  reappeared, but with their intensity enhanced compared to that observed prior to adsorption of  $\text{NH}_3$ . This indicates an increase in the concentration of  $\text{Pd}^+$  species following this treatment.

To elucidate the role of palladium in this system, identical time-resolved DRIFTS experiments were performed with a  $\text{V}_2\text{O}_5/\text{Al}_2\text{O}_3$  sample. It was found that the presence of palladium was not required for  $\text{NH}_x$  generation, as both  $\text{NH}_3$  and  $\text{NH}_4^+$  species accumulated on the  $\text{V}_2\text{O}_5/\text{Al}_2\text{O}_3$  sample in the presence of  $\text{H}_2 + \text{NO} + \text{O}_2$ . Figure 6 shows time-resolved spectra obtained following a switch to 500 ppm  $\text{NO} + 5\%\text{O}_2$  after the catalyst had been preconditioned in a flow containing 4000 ppm  $\text{H}_2 + 500\text{ ppm NO} + 5\%\text{O}_2$  for 1 h. Following the  $\text{H}_2 + \text{NO} + \text{O}_2$  treatment (spectrum at  $t = 0$ ),  $\text{NH}_3$  and  $\text{NH}_4^+$  species were again observed (bands at  $1282/1625\text{ cm}^{-1}$  and  $1420/1660\text{ cm}^{-1}$ , respectively). The negative band at  $2045\text{ cm}^{-1}$ , which indicates loss of  $\text{V}^{5+} = \text{O}$  species was also observed. However, the band at  $2189\text{ cm}^{-1}$  (possibly  $\text{N}_2^-$ ) was absent in this case, as was the  $1819\text{ cm}^{-1}$  feature (consistent with its assignment to a  $\text{Pd}^+ - \text{NO}$  species). The absence of these bands is likely to be related to the much lower activity of this sample. Comparison with figure 5 indicates that the concentration of Lewis acid sites relative to Brønsted acid sites was also somewhat diminished in the absence of palladium. Following the switch to 500 ppm  $\text{NO} +$

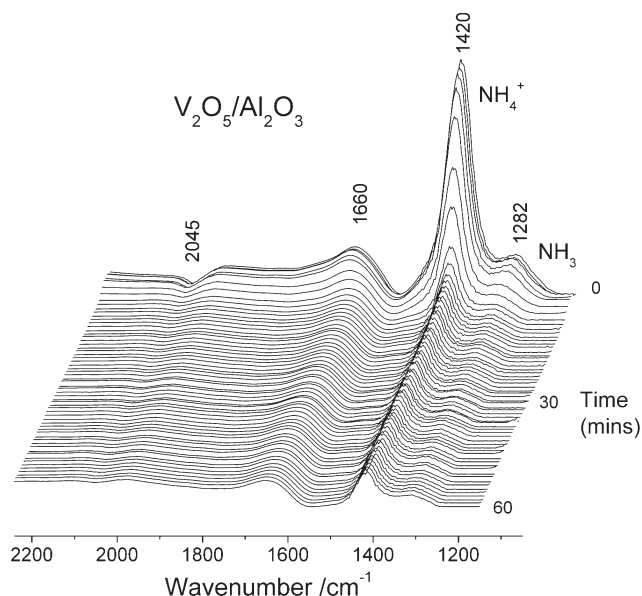


Figure 6. Time-resolved DRIFT spectra showing reactivity of NH<sub>3</sub> and NH<sub>4</sub><sup>+</sup> species in flowing NO + O<sub>2</sub> over V<sub>2</sub>O<sub>5</sub>/Al<sub>2</sub>O<sub>3</sub> at 250 °C (500 ppm NO + 5% O<sub>2</sub>).

5% O<sub>2</sub>, a very rapid decline in the intensity of NH<sub>3</sub> and NH<sub>4</sub><sup>+</sup> species was again observed.

Although support-bound NH<sub>3</sub> was rapidly consumed in flowing NO + O<sub>2</sub>, this purely support-mediated process was only a minor channel for NO<sub>x</sub> conversion over the Pd/V<sub>2</sub>O<sub>5</sub>/Al<sub>2</sub>O<sub>3</sub> catalyst. This is shown by the fact that the V<sub>2</sub>O<sub>5</sub>/Al<sub>2</sub>O<sub>3</sub> control sample displayed much lower activity under these conditions. An explanation is therefore required regarding the promoting influence of palladium in this system. One possibility is that palladium promotes NO oxidation to NO<sub>2</sub>, which subsequently reacts with adsorbed NH<sub>x</sub> species. It was observed, however, that whenever NH<sub>x</sub> were present on the V<sub>2</sub>O<sub>5</sub>/Al<sub>2</sub>O<sub>3</sub> surface, the corresponding Pd<sup>+</sup> – NO bands were removed (figures 3, 4, and 5). This may indicate rapid consumption of NO adsorbed on palladium sites by reaction with the NH<sub>x</sub> species generated on the support. The role of the noble metal may, therefore, be to catalyze this NO + NH<sub>x</sub> reaction. The participation of palladium in this process explains why the concentration of N<sub>2</sub>O produced, although relatively small, is still significantly higher than observed during conventional NH<sub>3</sub> SCR over V<sub>2</sub>O<sub>5</sub>/Al<sub>2</sub>O<sub>3</sub> [3,4].

#### 4. Conclusions

1. Pd/V<sub>2</sub>O<sub>5</sub>/Al<sub>2</sub>O<sub>3</sub> catalysts deliver very high NO<sub>x</sub> conversions (> 90%) in the presence of H<sub>2</sub> + NO + O<sub>2</sub> under oxygen-rich conditions. Very good nitrogen selectivity is also obtained (~80%).

2. The high activity is related to *in situ* formation of NH<sub>x</sub> species. Both NH<sub>3</sub> and NH<sub>4</sub><sup>+</sup> species are observed, with the latter dominant.

3. The formation of NH<sub>x</sub> species occurs on the V<sub>2</sub>O<sub>5</sub> component and does not involve participation of the noble metal. This support-generated NH<sub>x</sub> is able to react with NO species adsorbed on palladium sites.

#### References

- [1] V.I. Pârvulescu, P. Grange and B. Delmon, *Catal. Today* 46 (1998) 233.
- [2] A. Fritz and V. Pitchon, *Appl. Catal.*, B 13 (1997) 1.
- [3] G.T. Went, L.J. Leu, R.R. Rosin and A.T. Bell, *J. Catal.* 134 (1992) 492.
- [4] G. Busca, L. Lietti, G. Ramis and F. Berti, *Appl. Catal.*, B 18 (1998) 1.
- [5] M. Koebel, M. Elsener and M. Kleemann, *Catal. Today* 59 (2000) 335.
- [6] L.F. Xu, R.W. McCabe and R.H. Hammerle, *Appl. Catal.*, B 39 (2002) 51.
- [7] E. Seker, N. Yasyerli, E. Gulari, C. Lamert and R.H. Hammerle, *Appl. Catal.*, B 37 (2002) 27.
- [8] J.P. Breen, R. Burch and N. Lingaiah, *Catal. Lett.* 79 (2002) 171.
- [9] N. Macleod, R. Cropley and R.M. Lambert, *Catal. Lett.* 86 (2003) 69.
- [10] A. Ueda, N. Takayuki, A. Masashi and T. Kobayashi, *Catal. Today* 45 (1998) 135.
- [11] A. Ueda, T. Nakao, M. Azuma and T. Kobayashi, *Chem. Lett.* (1998) 595.
- [12] R. Burch and M.D. Coleman, *J. Catal.* 208 (2002) 435.
- [13] N. Macleod and R.M. Lambert, *Catal. Commun.* 3 (2002) 61.
- [14] N. Macleod, R. Cropley, J.M. Keel and R.M. Lambert, submitted to *J. Catal.*
- [15] N. Macleod, J. Isaac and R.M. Lambert, *J. Catal.* 193 (2000) 115.
- [16] W.S. Kijlstra, D.S. Brand, E.K. Poels and A. Blik, *J. Catal.* 171 (1997) 208.
- [17] F.C. Meunier, J.P. Breen, V. Zuzaniuk, M. Olsson and J.R.H. Ross, *J. Catal.* 187 (1999) 493.
- [18] S. Kameoka, Y. Ukisu and T. Miyadera, *Phys. Chem. Chem. Phys.* 2 (2000) 367.
- [19] K.I. Hadjiivanov, *Catal. Rev.-Sci. Eng.* 42 (2002) 71.
- [20] R.Q. Long and R.T. Yang, *J. Catal.* 196 (2000) 73.
- [21] M.A. Centeno, I. Carrizosa and J.A. Odriozola, *Phys. Chem. Chem. Phys.* 1 (1999) 349.
- [22] N.Y. Topsøe, H. Topsøe and J.A. Dumesic, *J. Catal.* 151 (1995) 226.
- [23] T. Mailet, J. Barbier, P. Gelin, H. Praliaud and D. Duprez, *J. Catal.* 202 (2001) 367.
- [24] K. Almusaiteer and S.S.C. Chuang, *J. Catal.* 184 (1999) 189.
- [25] H. Miyata, S. Konishi, T. Ohno and F. Hatayama, *J. Chem. Soc. Faraday Trans.* 9 (1995) 1557.
- [26] N.Y. Topsøe, *J. Catal.* 128 (1991) 499.
- [27] M.A. Centeno, I. Carrizosa and J.A. Odriozola, *Appl. Catal.*, B 29 (2001) 307.
- [28] H. Schneider, S. Tschudin, M. Schneider, A. Wokaun and A. Baiker, *J. Catal.* 147 (1994) 5.
- [29] H. Kamata, K. Takahashi and C.U.I. Odenbrand, *J. Catal.* 185 (1999) 106.
- [30] G. Ramis, G. Busca, V. Lorenzelli and P. Forzatti, *Appl. Catal.*, 64 (1990) 243.
- [31] G. Ramis, L. Yi, G. Busca, M. Turco, E. Kotur and R.J. Willey, *J. Catal.* 157 (1995) 523.
- [32] M.A. Centeno, I. Carrizosa and J.A. Odriozola, *Appl. Catal.*, B 19 (1998) 67.
- [33] N.Y. Topsøe, H. Topsøe and J.A. Dumesic, *J. Catal.* 151 (1995) 241.
- [34] J.M.G. Amores, V.S. Escribano, G. Ramis and G. Busca, *Appl. Catal.*, B 13 (1997) 45.